Journal of Power Sources 196 (2011) 10314–10321

Contents lists available at ScienceDirect

Journal of Power Sources

journal homepage: www.elsevier.com/locate/jpowsour

Prognostics of lithium-ion batteries based on Dempster–Shafer theory and the Bayesian Monte Carlo method

Wei He, Nicholas Williard, Michael Osterman, Michael Pecht*

Center for Advanced Life Cycle Engineering, University of Maryland, College Park, MD 20742, USA

ARTICLE INFO

Article history:
Received 7 June 2011
Received in revised form 4 August 2011
Accepted 6 August 2011
Available online 12 August 2011

Keywords:
Lithium-ion batteries
State of health
Remaining useful life
Dempster–Shafer theory
Bayes updating
Monte Carlo

ABSTRACT

A new method for state of health (SOH) and remaining useful life (RUL) estimations for lithium-ion batteries using Dempster–Shafer theory (DST) and the Bayesian Monte Carlo (BMC) method is proposed. In this work, an empirical model based on the physical degradation behavior of lithium-ion batteries is developed. Model parameters are initialized by combining sets of training data based on DST. BMC is then used to update the model parameters and predict the RUL based on available data through battery capacity monitoring. As more data become available, the accuracy of the model in predicting RUL improves. Two case studies demonstrating this approach are presented.

1. Introduction

Lithium-ion batteries are a common energy solution for many types of systems including consumer electronics, electric vehicles, and military and aerospace electronics, due to their high energy density, high galvanic potential, lightness of weight, and long lifetime compared to lead–acid, nickel–cadmium, and nickel–metal–hydride cells [1,2]. The degradation of a lithium-ion battery can be characterized by the decrease in capacity over repeated charge cycles. Capacity is the amount of electrical charge a battery can hold in its fully charged state. For many applications, failure is considered to occur when the capacity of the battery is reduced to below 80% of its rated value [3,4]. At this point, the battery is considered to be an unreliable power source and should be replaced, because it tends to exhibit an exponential decay of capacity after it passes this point.

Failure of a battery could lead to loss of operation, reduced capability, downtime, and even catastrophic failure. For example, in April 2000 a battery failure resulted in an electrical malfunction that disabled normal landing gear extension capability and led to the crash of a plane during landing. Another battery failure caused the loss of the Mars global surveyor in November 2006. In this case, the surveyor's batteries were exposed to sunlight, and the high temperature resulted in the premature depletion of the batteries. Recently, a survey conducted by Emerson Network Power showed that one of the biggest causes of data center downtime is uninterruptible power supply (UPS) battery failures. For data centers, one hour of downtime could lead to tens of thousands of dollars in losses.

Prognostics and health management (PHM) is an enabling discipline consisting of technologies and methods to assess the reliability of a product in its actual life cycle conditions to determine the advent of failure and mitigate system risk [5]. With a PHM system for batteries in place, maintenance decisions can be made on a conditional basis and users can be given ample forewarning before a failure occurs so that risk factors can be mitigated. PHM comes in two main approaches: physics-of-failure (PoF) and data-driven. PoF-based prognostic methods utilize knowledge of a product's life cycle loading conditions, geometry, material properties, and failure mechanisms to estimate its remaining useful life (RUL) [6,7]. Data-driven techniques extract features from performance data such as current, voltage, time, and impedance, using statistical and machine learning techniques to track the product's degradation and estimate its RUL [8]. Data-driven methods do not require specific knowledge of material properties, constructions, or failure mechanisms [9], and avoid developing high-level physical models of the system, so that they are less complex than PoF based approaches. Data-driven methods can capture the inherent relationships and learn trends present in the data to provide RUL predictions.

Kozlowski [10] proposed a data-driven prognostic approach that combines three predictors— auto-regressive moving average (ARMA), neural networks, and fuzzy-logic— to predict the RUL of

* Corresponding author. Tel.: +1 301 405 5323; fax: +1 301 314 9269.
E-mail address: pecht@calce.umd.edu (M. Pecht).

0378-7753/$ – see front matter © 2011 Elsevier B.V. All rights reserved.
doi:10.1016/j.jpowsour.2011.08.040

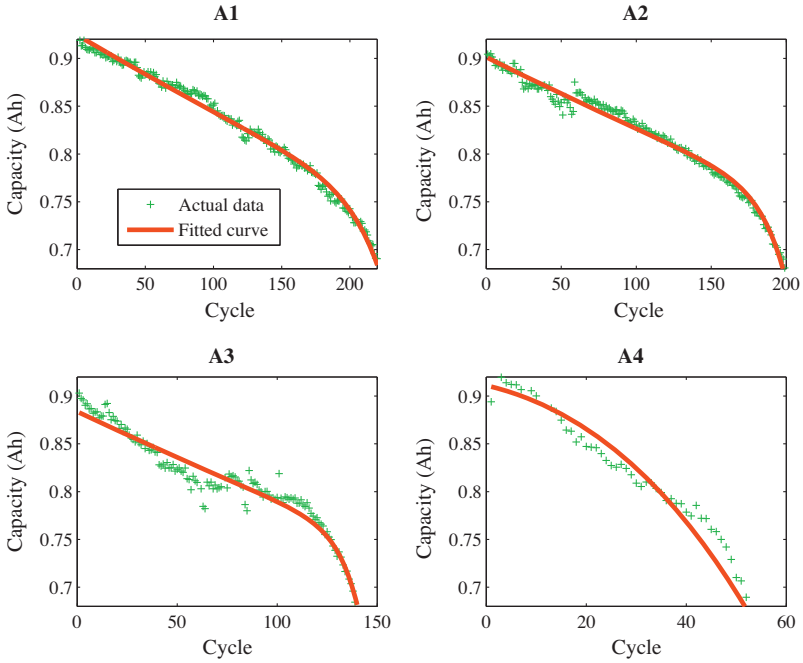

Fig. 1. The curve fitting of the model Eq. (1) to the type A battery data.

batteries. These predictors were trained by the data sets of batteries of the same size and chemistry under various loading conditions. However, collecting training data that has good coverage over all the possible loading conditions can be time consuming and expensive. Burgess proposed a method to estimate the RUL for valve regulated lead–acid batteries based on capacity measurements and Kalman filtering [11]. The capacity fade trend is divided into two phases: a slowly decreasing phase followed by a much more rapid decreasing phase. When the battery capacity falls to the second phase, the Kalman filter is trigged to give predictions of RUL based on a probabilistic capacity fade model. However, the duration of the second phase of battery capacity fade is very short compared to the whole battery life, so this approach cannot give predictions at an early time of a battery's life. Saha et al. [12,13] used the relevance vector machine (RVM) and a particle filter to predict RUL of lithium-ion batteries. In their method, RVM was employed to learn the non-linear patterns in data, and particle filter is used to estimate the RUL with a state-space model based on impedance spectroscopy data. This approach shows good accuracy. However, the impedance measurement requires expensive and bulky equipment and is time consuming. In addition, the battery should be disconnected from the charger or load during the measurement. These shortcomings confine its implementation in on-board applications.

To solve these problems, a new battery PHM approach is proposed in this paper, aiming at on-board applications and RUL predictions from an early point in the battery's life. Based on data analysis, a new model consisting of two exponential functions is developed to model the battery capacity fade. This model has a good balance between the modeling accuracy and complexity, and can accurately capture the non-linearity of the battery capacity fade trend. In order to achieve accurate prediction from an early point in life, two algorithms are used to make the model parameters quickly adapt to a specific battery system and loading condition. The first step is an initial model parameter selection based on the Dempster–Shafer theory (DST) [14,15]. The DST is an effective data fusion method. It has a lot of applications in sensor information fusion [16–18], expert opinion combination, and classifier combination [19–21]. DST allows one to gather the information from available battery data to elicit the initial model parameters with the highest degree of belief. The second step is the Bayesian Monte Carlo (BMC) [22–24], which is used to update the model parameters based on new measurements. With the tuned parameters obtained by BMC, the capacity fading model can be extrapolated to provide the SOH and RUL predictions. It will be shown in the case studies that BMC can give more accurate parameter estimations than the extended Kalman filter (EKF). Compared to traditional battery RUL prognostic methods, like those in Refs. [10–13], the advantages of the proposed battery prognostic approach are: the ability to provide accurate prediction from an early point of the battery's life, no need for a large amount of training data, and the potential application to on-board battery PHM systems.

This paper is organized as follows. Section 2 introduces the battery capacity degradation model developed in this study. Section 3 discusses the uncertainties in the battery degradation process. Section 4 introduces the Dempster–Shafer theory and its application to initial model parameter selection. Section 5 introduces the theory for the Bayesian Monte Carlo. Section 6 presents the algorithm for the remaining useful life calculation. Section 7 presents the application of the proposed approach to battery prognostics. Conclusions are drawn in Section 8.

2. Capacity degradation model

As a battery ages, the maximum available capacity of it will decrease. To investigate the capacity fade, two types of commercialized lithium-ion batteries were tested. The first type (type A) has a rated capacity of 0.9 Ah, and the second type (type B) has a rated capacity of 1.1 Ah. Both types of batteries have a graphite anode and a lithium cobalt oxide cathode which were verified using electron dispersive spectroscopy (EDS). The cycling of the batteries was accomplished by multiple charge–discharge tests using an Arbin BT2000 battery testing system under room temperature. The discharge current for the type A batteries was 0.45 A, and for type B batteries it was 1.1 A. The charging and discharging of the batteries were cut off at the manufacturer's specified cutoff voltage. The capacity of the tested batteries was estimated using the Coulomb counting method, since full charge–discharge cycles were

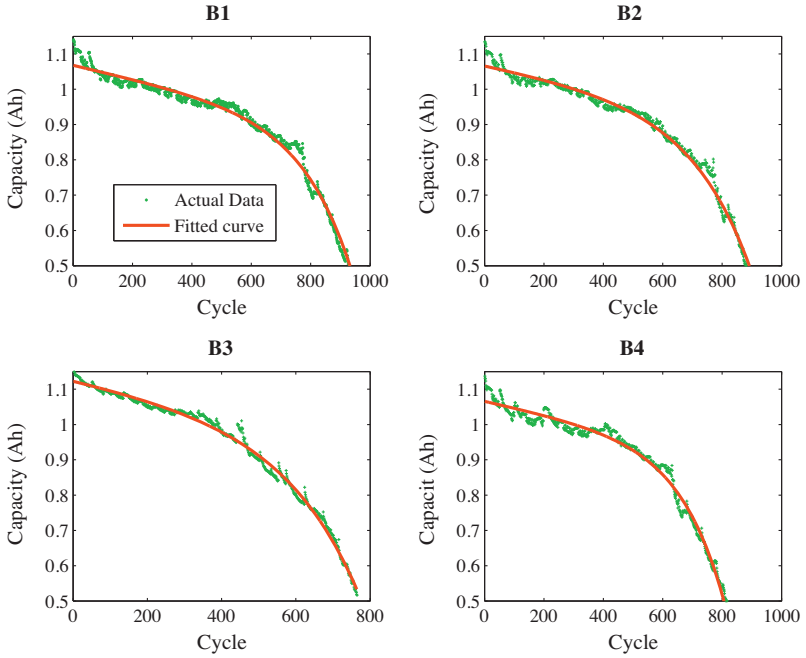

Fig. 2. The curve fitting of the model Eq. (1) to the type B battery data.

conducted. In actual practice, batteries may not always run from a fully charged state to a fully discharged state. In industrial applications, a common practice in battery management is to conduct the capacity test regularly to monitor the capacity fade and determine whether the battery requires replacement [4,11]. The capacity data obtained by capacity testing can be used to predict the battery's SOH and RUL based on the proposed approach in this paper. There also exist some advanced techniques that can be used to estimate capacity from partial discharge data, such as the EKF based method [25] and total least square method [26]. For more information about the capacity estimation methods, readers can refer to Ref. [27], in which several capacity estimation methods were reviewed.

The capacity fading trends of the two types of batteries are shown in Figs. 1 and 2 respectively. It can be seen that the capacity fade occurs in a near linear fashion followed by a pronounced reduction. The loss of capacity is often brought on by side reactions that occur between the battery's electrodes and electrolyte which consume lithium, thus removing it from the Faradic process. Solid precipitates arise as the product of these side reactions and adhere to the electrodes, increasing the internal resistance of the cell. The combined effects of these reactions reduce the battery's ability to store electrical energy [3,28,29]. Fig. 3 shows the impedance spectroscopy measurements for the battery A3. It can be seen that the Nyquist plots show a dramatic rise in the electrolytic resistance, charge transfer resistance, and the double layer capacitance with increased cycling based on the Randles model. This points to increased resistance of the solid–electrolyte interface (SEI) layer as well as decomposition of the electrolyte as the reason for capacity fade. Refs. [13,30] used the sum of exponential functions to model the increase of internal impedance due to SEI thickening with time. As battery capacity fade is closely related to the internal impedance increase, potential models for capacity fade can also be exponential models. Based on regression analysis of experimental data, it is found that a model in the following form can well describe the capacity fade trend of many different batteries:

$$Q = a \cdot \exp(b \cdot k) + c \cdot \exp(d \cdot k) \quad (1)$$

where Q is the capacity of the battery; k is the cycle number; the parameters a and b can be related to the internal impedance; and c and d stand for the aging rate.

To demonstrate the suitability of the model in Eq. (1) in depicting battery degradation, Figs. 1 and 2 show the curve fitting result (solid line) of Eq. (1) to the capacity data of type A and type B batteries, respectively. The model parameters were estimated by the curve fitting tool in Matlab. To quantify the performance of the model, the goodness-of-fit statistics [31] are shown in Table 1. The root mean squared errors (RMSE) are close to 0 while the R^2 and adjusted R^2 are near to 1. These statistical parameters indicate that the proposed model is suitable to represent the capacity fade data.

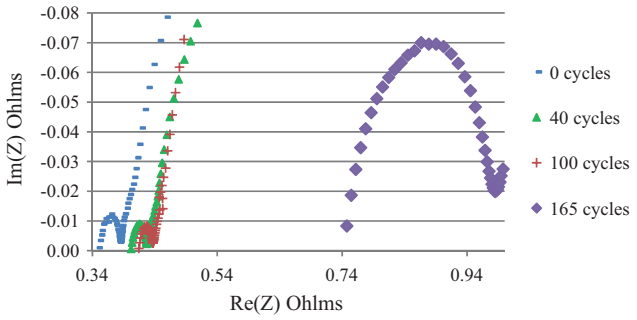

Fig. 3. The impedance spectroscopy measurements for the battery A3 at different cycles.

Table 1
Goodness of fit statistics.

Battery ID	R^2	Adjusted R^2	RMSE
A1	0.9948	0.9947	0.0049
A2	0.9912	0.9911	0.0055
A3	0.9537	0.9527	0.0114
A4	0.9869	0.9861	0.0084
B1	0.9909	0.9909	0.0190
B2	0.9889	0.9889	0.0202
B3	0.9924	0.9924	0.0136
B4	0.9929	0.9929	0.0203

3. Uncertainties in battery prognostics

In this study, the battery degradation is modeled by Eq. (1). This model can be well fit to each battery, as shown in Figs. 1 and 2. However, it is easy to see that there can be large discrepancies between each sample's degradation trends. These variations can arise from several sources: (1) Inherent system uncertainties: because of the uncertainties in the manufacturing assemblies and material properties, batteries may have different initial capacities, which can be observed from Fig. 1. Each battery may also be individually affected by impurities or defects, which may lead to different aging rates. (2) Measurement uncertainties: uncertainties are likely to arise from background noise of measurement devices and from system process noise. (3) Operation environment uncertainties: the rate of capacity fade can be affected by usage conditions such as the ambient temperature, discharge current rate, depth of discharge, and aging periods. (4) Modeling uncertainties: the regression model is an approximation of the battery degradation, which will result in some modeling error.

In the degradation in Eq. (1), the parameters a and c characterize the initial capacity, meanwhile the parameters b and d represent the aging rate. If the model parameters are inaccurately defined, errors will occur in the prediction. Uncertainty management tools are needed to account for the noise or errors in capacity estimations, the variations in battery chemistries and loading conditions, etc. Therefore, the DST and BMC are adopted to ensure that the proposed degradation model adapts to a specific battery system and loading condition. The final RUL prediction can be obtained in the form of a probability density function so that the confidence level of the prediction can be assessed.

4. Model initialization using Dempster–Shafer theory

To provide accurate predictions from an early point in life, it is critical that these model parameters are well representative of the true physical response of the battery. The available battery data can be used to initialize these parameters. A good combination of the initial parameters will shorten the convergence time of the model to the real system respond. Here, we use the mixing combination rule of the Dempster–Shafer theory to get the basis, or the "prior model", for the BMC updating. The mixing combination rule was proposed to combine evidence based on the belief measure of each data set [15]. It assumes that if two bodies of evidence agree, they should be given a higher value of belief and hence weigh more when combining each of the pieces of evidence together [32]. The detailed steps of DST in initializing model parameters are illustrated as follows using the data from batteries A1, A2, and A3.

First, the Gauss–Newton algorithm in the Matlab curve fitting tool was used to fit the proposed model to each subset of data in the training set. These fits produced the parameter estimations with 95% confidence bounds shown in Table 2.

Next, each of the parameters from the respective data sets, expressed through confidence intervals, were compared in order to calculate the belief measure associated with each parameter. Initially, because we assume all sources to be equally credible; the basic belief assignment, which assesses the likelihood of each set, is given an equal value:

$$m(A_i) = \frac{1}{n} \tag{2}$$

where $m(A_i)$ is the basic belief assignment for a set A_i and n is the number of sets in the training set family. Since 3 training data sets were used, the initial basic belief assignment for each data set is 0.333. By using this as a starting point we can calculate the belief measure of each parameter. The belief measure $Bel(A_i)$ for a set A_i is

Table 2
Fitted parameters from each set of training data, including the bounds for the 95% confidence intervals.

Battery ID	Parameter	Low bound	Mean	Upper bound
A1	a	−1.660E−03	−1.042E−03	−4.240E−04
	b	2.068E−02	2.268E−02	2.467E−02
	c	9.079E−01	9.190E−01	9.301E−01
	d	−1.210E−03	−1.035E−03	−8.600E−04
A2	a	−2.007E−06	−9.860E−07	3.442E−08
	b	5.283E−02	5.752E−02	6.221E−02
	c	8.931E−01	8.983E−01	9.035E−01
	d	−9.007E−04	−8.340E−04	−7.670E−04
A3	a	−3.788E−05	−1.530E−05	7.272E−06
	b	5.398E−02	6.296E−02	7.193E−02
	c	8.631E−01	8.757E−01	8.883E−01
	d	−1.188E−03	−9.400E−04	−6.920E−04

Table 3
Belief values for each parameter.

Battery ID	a	b	c	d
A1	0.333	0.333	0.333	0.333
A2	0.333	0.333	0.333	0.333
A3	0.666	0.333	0.333	0.666

defined as the sum of all the basic belief assignments of the subsets of the set of interest:

$$Bel(A_i) = \sum_{all\, A_j \subseteq A_i} m(A_j) \tag{3}$$

Eq. (3) implies that we must consider parameter intervals that are subsets of other parameter intervals in order to compute the belief measure. Take the parameter a for example, In Table 2 the parameter interval of A3 contains that of A2. As a result, the belief value of A3 for the parameter a is 0.333 + 0.333 = 0.666. This analysis provides us with the following belief values for each of the parameters from the training data set family shown in Table 3. Now that the belief measures have been evaluated for each parameter, we can go back and update the basic belief assignments from the belief measure with the following inverse function,

$$m(A_i) = \sum_{all\, A_j \subseteq A_i} (-1)^{|A_i - A_j|} Bel(A_j) \tag{4}$$

where $|A_i - A_j|$ is the difference of the cardinality of the two sets. When computing the cardinality of each parameter set, the Lebesgue measure must be used, because each interval was defined only by its upper and lower bounds and is therefore uncountable. However, because the intervals are so small, and the sizes of the intervals are relatively similar, the difference in cardinalities between A_i and A_j can be considered zero. Therefore, the assignment conversion for this special case can be approximated by:

$$m(A_i) \approx \sum_{all\, A_j \subseteq A_i} Bel(A_j) \tag{5}$$

Using this to convert back to the basic belief assignment, and then normalizing these assignments, the values for m can be obtained as

Table 4
Basic assignments for each parameter value.

Battery ID	a	b	c	d
A1	0.2	0.333	0.333	0.2
A2	0.2	0.333	0.333	0.2
A3	0.6	0.333	0.333	0.6

shown in Table 4. Now each parameter can be combined using the weighted arithmetic mean:

$$CP = \sum_{i=1}^{3} m(A_i)h(A_i) \tag{6}$$

where $h(A_i)$ is the estimated parameter from training data A_i, CP is the combined parameter from the initial model, and $m(A_i)$ are the basic belief assignments or the weight factor. This gives us the following combined parameter values:

$$\begin{aligned} a &= -0.00022 \\ b &= 0.04772 \\ c &= 0.89767 \\ d &= -0.00094 \end{aligned} \tag{7}$$

5. Model updating via Bayesian Monte Carlo

Once the initial parameter values are determined and capacity data are collected, the parameters can be updated based on Bayes'rule. The estimation of the parameters will gradually converge to their true values as more and more capacity data becomes available.

To model the uncertainty as discussed above, it is assumed that the parameters: a, b, c, and d, as well as the error of the regression model, are subject to Gaussian distribution:

$$\begin{aligned} a_k &= a_{k-1} + \omega_a \quad \omega_a \sim \mathcal{N}(0, \sigma_a) \\ b_k &= b_{k-1} + \omega_b \quad \omega_b \sim \mathcal{N}(0, \sigma_b) \\ c_k &= c_{k-1} + \omega_c \quad \omega_c \sim \mathcal{N}(0, \sigma_c) \\ d_k &= d_{k-1} + \omega_d \quad \omega_d \sim \mathcal{N}(0, \sigma_d) \end{aligned} \tag{8}$$

$$Q_k = a_k \cdot \exp(b_k \cdot k) + c_k \cdot \exp(d_k \cdot k) + v \quad v \sim \mathcal{N}(0, \sigma_Q) \tag{9}$$

where Q_k is the capacity measured at cycle k, and $\mathcal{N}(0, \sigma)$ is Gaussian noise with zero mean and standard deviation σ.

The initial values a_0, b_0, c_0, and d_0 are set as the weighted sum of the model parameters obtained from the training data based on DST. For convenience, we denote $\boldsymbol{X}_k = [a_k, b_k, c_k, d_k]$ as the parameter vector at cycle k. The goal of this study is to estimate the probability distribution $P(\boldsymbol{X}_k|\boldsymbol{Q}_{0:k})$ of the parameter vector $\boldsymbol{X}_k$ given a series of capacity measurements: $\boldsymbol{Q}_{0:k} = [Q_0, Q_1, \ldots, Q_k]$. Within a Bayesian framework, the posterior distribution $P(\boldsymbol{X}_k|\boldsymbol{Q}_{0:k})$ can be recursively computed by two steps: prediction and update. Given the probability distribution $P(\boldsymbol{X}_{k-1}|\boldsymbol{Q}_{0:k-1})$ at cycle $k-1$, the prediction stage involves using the model (8) to obtain the prior probability distribution of $\boldsymbol{X}_k$ via the Chapman–Kolmogorov equation:

$$P(\boldsymbol{X}_k|\boldsymbol{Q}_{0:k-1}) = \int P(\boldsymbol{X}_k|\boldsymbol{X}_{k-1}) P(\boldsymbol{X}_{k-1}|\boldsymbol{Q}_{0:k-1})\, d\boldsymbol{X}_{k-1} \tag{10}$$

At cycle k, a new observation Q_k is obtained and used to update the prior distribution via Bayes'rule [22,23], so as to obtain the required posterior distribution of $\boldsymbol{X}_k$ as follows:

$$P(\boldsymbol{X}_k|\boldsymbol{Q}_{0:k}) = \frac{P(\boldsymbol{X}_k|\boldsymbol{Q}_{0:k-1})\, P(Q_k|\boldsymbol{X}_k)}{P(Q_k|\boldsymbol{Q}_{0:k-1})} \tag{11}$$

where the normalizing constant is:

$$P(Q_k|\boldsymbol{Q}_{0:k-1}) = \int P(\boldsymbol{X}_k|\boldsymbol{Q}_{0:k-1}) P(Q_k|\boldsymbol{X}_k)\, d\boldsymbol{X}_k \tag{12}$$

The recurrence relation between Eqs. (10) and (11) forms the basis for the exact Bayesian solution [22,23]. However, this recursive propagation of the posterior density is only a conceptual solution in general. It is hard to analytically evaluate these distributions, because they require the evaluation of complex high-dimensional integrals [22]. However, it is possible to approximately and numerically solve this Bayesian updating problem by adopting Monte Carlo sampling [22,23]. The key idea is to represent the probability density function (PDF) by a set of random samples with associated weights and compute estimates based on these samples and weights as below:

$$P(\boldsymbol{X}_k|\boldsymbol{Q}_{0:k}) \approx \sum_{i=1}^{N} \omega_k^i \delta(\boldsymbol{X}_k - \boldsymbol{X}_k^i) \tag{13}$$

where $\boldsymbol{X}_k^i$, $i = 1, 2, 3, \ldots, N$, is a set of independent random samples drawn from $P(\boldsymbol{X}_k|\boldsymbol{Q}_{0:k})$; ω_k^i is the Bayesian importance weight associated with each sample $\boldsymbol{X}_k^i$; and $\delta(\cdot)$ is the Dirac delta function. In practice, $P(\boldsymbol{X}_k|\boldsymbol{Q}_{0:k})$ is usually unknown. In this case, one can resort to importance sampling, i.e., to sample $\boldsymbol{X}_k^i$ from an arbitrarily chosen distribution $\pi(\boldsymbol{X}_k^i|\boldsymbol{Q}_{0:k})$ called the importance function. Then the estimate of ω_k^i can be obtained by [22–24]:

$$\omega_k^i = \frac{P(\boldsymbol{Q}_{0:k}|\boldsymbol{X}_k^i)\, P(\boldsymbol{X}_k^i)}{\pi(\boldsymbol{X}_k^i|\boldsymbol{Q}_{0:k})} \tag{14}$$

The weight should be normalized by:

$$\omega_k^i = \frac{\omega_k^i}{\sum_{j=1}^{N} \omega_k^j} \tag{15}$$

A recursive formula for updating the weights can be obtained by [24]:

$$\omega_k^i = \omega_{k-1}^i \frac{P(Q_k|\boldsymbol{X}_k^i)\, P(\boldsymbol{X}_k^i|\boldsymbol{X}_{k-1}^i)}{\pi(\boldsymbol{X}_k^i|\boldsymbol{X}_{k-1}^i, \boldsymbol{Q}_{0:k})} \tag{16}$$

If the importance function is chosen by $\pi(\boldsymbol{X}_k^i|\boldsymbol{X}_{k-1}^i, \boldsymbol{Q}_{0:k}) = P(\boldsymbol{X}_k^i|\boldsymbol{X}_{k-1}^i)$, then the weight updating rule becomes:

$$\omega_k^i = \omega_{k-1}^i P(Q_k|\boldsymbol{X}_k^i) \tag{17}$$

As the number of Monte Carlo sampling $N \to \infty$, the approximation Eq. (13) approaches the true posterior density $P(\boldsymbol{X}_k|\boldsymbol{Q}_{0:k})$.

6. The SOH prognostics and RUL estimation

Using the Bayesian Monte Carlo approach, the parameter vector can be updated at each cycle. In the updating procedure, N samples are used to approximate the posterior PDF. Each sample represents a candidate model vector $\boldsymbol{X}_k^i$, $i = 1, 2, \ldots, N$, so the prediction of Q will have N possible trajectories with the corresponding importance weights ω_k^i. Then, the h-step ahead prediction of each trajectory at cycle k can be calculated by:

$$Q_{k+h}^i = a_k^i \cdot \exp[b_k^i \cdot (k+h)] + c_k^i \cdot \exp[d_k^i \cdot (k+h)] \tag{18}$$

The estimated posterior PDF of the prediction can be obtained by the prediction at each trajectory with associated weights:

$$P(Q_{k+h}|\boldsymbol{Q}_{0:k}) \approx \sum_{i=1}^{N} \omega_k^i \delta(Q_{k+h} - Q_{k+h}^i) \tag{19}$$

The expectation or mean of the h-step ahead prediction at the cycle k is given by:

$$\overline{Q}_{k+h} = \sum_{i=1}^{N} \omega_k^i Q_{k+h}^i \tag{20}$$

Since the failure threshold is defined as 80% of the rated capacity, the RUL estimation L_k^i of the ith trajectory at the cycle k can be obtained by solving the following equation:

$$a_k^i \cdot \exp[b_k^i \cdot (k + L_k^i)] + c_k^i \cdot \exp[d_k^i \cdot (k + L_k^i)] = 0.8 Q_{rated} \tag{21}$$

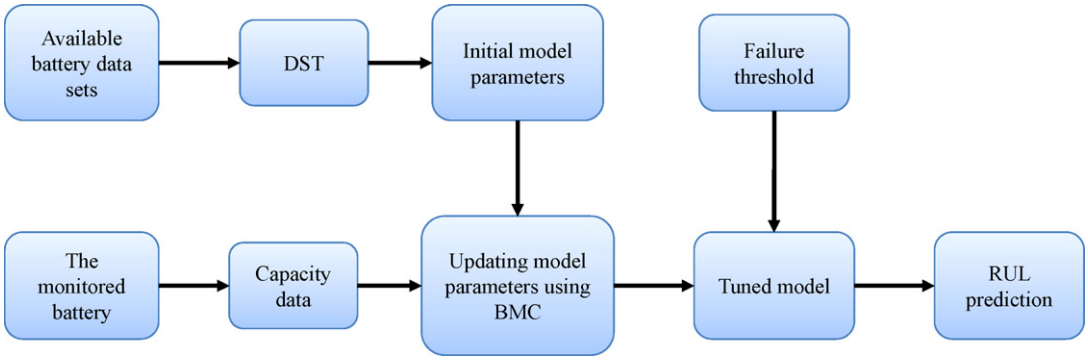

Fig. 4. The flowchart of the proposed scheme for battery prognostics.

Then, the distribution of RUL at the cycle k can be approximated by:

$$P(L_k|\mathbf{Q}_{0:k}) \approx \sum_{i=1}^{N} \omega_k^i \delta(L_k - L_k^i) \tag{22}$$

The expectation or mean of the RUL prediction at cycle k is given by:

$$\bar{L}_k = \sum_{i=1}^{N} \omega_k^i L_k^i \tag{23}$$

As a summary, Fig. 4 presents the flowchart of the proposed prognostic scheme. First, DST is used to combine the available battery data sets so as to get a starting point for BMC updating. As the capacity measurements of the monitored battery become available, model parameters are updated by BMC to track the degradation trend of the battery. The RUL prediction can be made by extrapolating the model to the failure threshold.

7. Prognostic results

In this section, two case studies are conducted to validate the proposed approach. In the first case study, the data from A1, A2 and A3 are used to elicit the initial model by the DST. A4, which shows the largest difference in its capacity fade trend compared to the other three batteries, is used as the testing sample to validate the proposed algorithm. Similarly, in the second case study, initial model parameters are selected based on B1, B2, and B3, and B4 is used for testing. The error of the mean RUL estimation and the standard deviation (SD) of the RUL estimation are used to quantify the performance of the proposed methodology.

The prognostic results for A4 at 18 cycles are shown in Fig. 5, where only data from the first 18 cycles are used to update the model. The error of the mean RUL prediction is 1 cycle, and the SD of the estimated RUL is 6 cycles. Fig. 6 presents the prediction result of A4 at 32 cycles. Since more data are available to update the model parameters, the accuracy of the mean RUL prediction is improved as the predicted failure cycle matches with the real value, and the SD of the RUL prediction is reduced to 2 cycles, meaning that the confidence level of the prediction increases.

Fig. 7 shows the prognostic results for battery B4 at 250 cycles. The predictions in the solid line well capture the non-linear fade trend of battery capacity. The prediction error of the failure cycle is 7 cycles away from the actual failure cycle, and the SD of the RUL prediction is 35 cycles. Based on the RUL PDF, the 95% confidence bound of the predicted failure cycle can be obtained as 550–670 cycles.

To demonstrate the effectiveness of DST in aggregating information from training data, comparison studies were conducted between DST and a mean averaging approach. In the mean averaging approach, the initial parameters are defined by the average of each parameter from each training data set and are used as the starting point for BMC updating. The prediction results of the mean averaging approach for A4 at 18 cycles and B4 at 250 cycles are shown in Figs. 8 and 9, respectively. In Fig. 8, the prediction error and SD are 4 and 12 respectively, which are greater than those

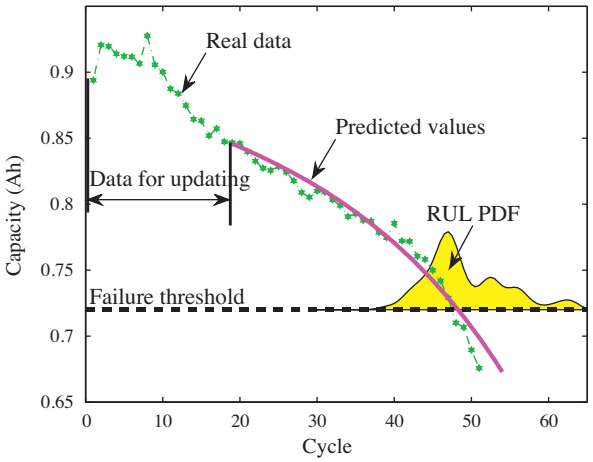

Fig. 5. Prediction result at 18 cycles for the battery A4. The BMC prediction model was initialized by DST. The prediction error is 1 cycle, and the standard deviation of RUL estimation is 6 cycles.

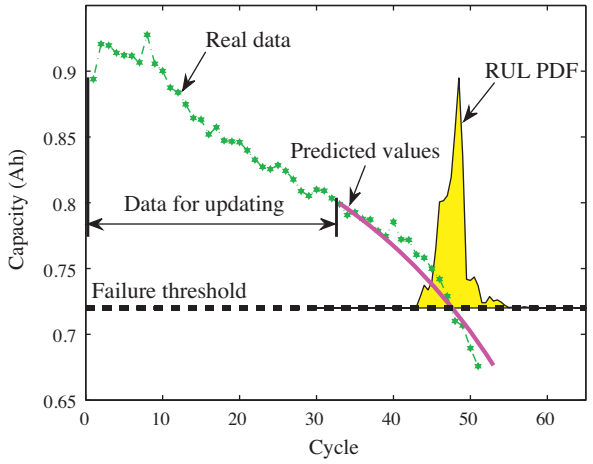

Fig. 6. Prediction result at 32 cycles for the battery A4. The BMC prognostic model was initialized by DST. BMC accurately predicted the failure time. The standard deviation of the RUL estimation is 2 cycles.

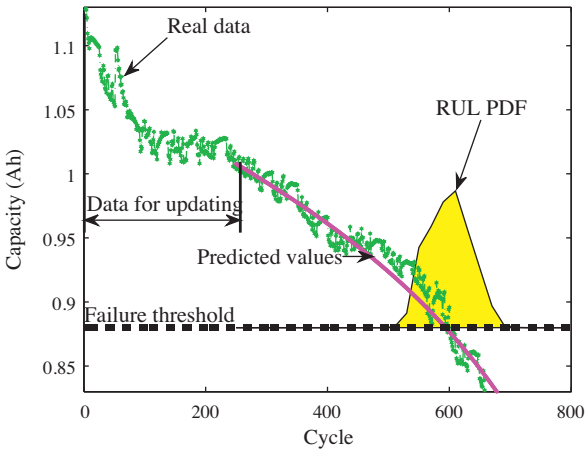

Fig. 7. Prediction results at 250 cycles for the battery B4. The BMC prognostic model was initialized by DST. The prediction error is 7 cycles, and the standard deviation of the RUL estimation is 35 cycles.

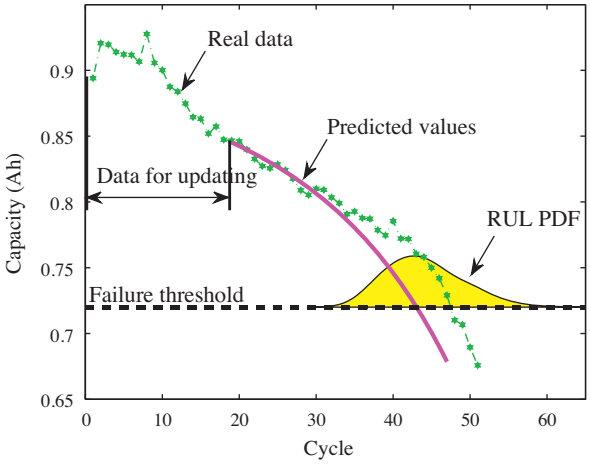

Fig. 8. Prediction results at 18 cycles for the battery A4. The initial model parameters were defined by the mean averaging approach. The prediction error is 4 cycles, and the standard deviation of the RUL estimation is 12 cycles.

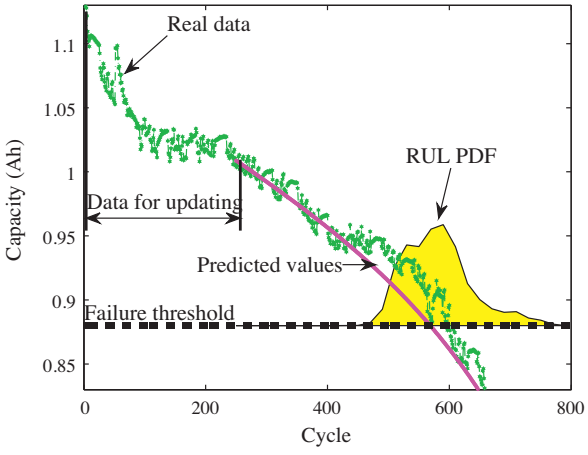

Fig. 9. Prediction results at 250 cycles for the battery B4. The initial model parameters were defined by the mean averaging approach. The prediction error is 31 cycles, and the standard deviation of the RUL estimation is 62 cycles.

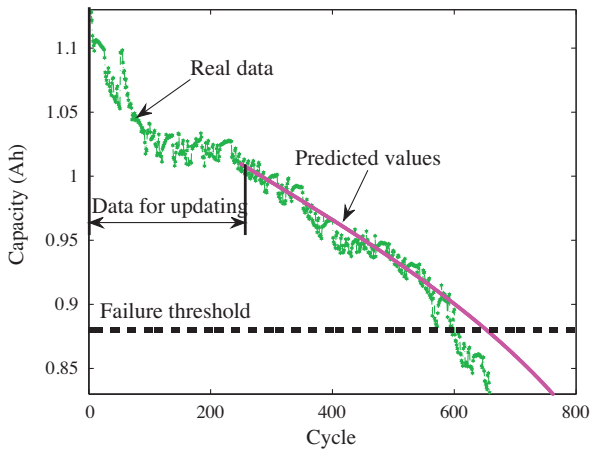

Fig. 10. Prediction results at 250 cycles for the battery B4 using extended Kalman filtering. The prediction error is 52 cycles.

obtained by using the DST (Fig. 5). In Fig. 9, the prediction error is 31 cycles. It is 24 cycles larger than the prediction error obtained by the DST. In addition, the SD of the RUL estimation in Fig. 9 is 62 cycles, which is 27 cycles larger than that obtained by the DST (Fig. 7). Therefore, the DST has been shown to be effective in fusing the available training data to provide the optimal initial parameters to start the BMC updating.

To compare the performance of the BMC with EKF, Fig. 10 shows the prediction results based on EKF for the battery B4. The degradation model and initial parameters used in EKF are the same as those used in BMC. In Fig. 10, the EKF over-predicted the failure cycle of the battery, and the prediction error of the failure cycle is 52 cycles, which is greater than that obtained by BMC by 45 cycles.

The BMC approach is computationally efficient. In the case study, 1000 samples were used in the BMC. The computational time of the BMC parameter updating at each cycle was within 10 ms using an Intel Core i7 M60 2.67 GHz processor and 4 Gb RAM under a Matlab 2010 environment.

8. Conclusions

Analysis of lithium-ion battery data shows that capacity fade can be modeled by the sum of two exponential functions of discharge cycles. RUL predictions can then be made by extrapolating the capacity fade model to the failure threshold. To estimate the model parameters and predict the RUL, a data-driven approach based on the DST and BMC was developed. The DST was used to select the initial model parameters for the BMC parameter estimation. The BMC is a combination of Monte Carlo and Bayesian updating. In the BMC algorithm, a set of possible degradation trajectories are simulated based on the capacity fade model. Each trajectory is then assigned a weight according to its conformity to the capacity measurements using the Bayesian rule. The model parameters are estimated as the weighted sum of the model parameters defined by each trajectory. The RUL PDF is approximated by the RUL estimation at each simulated degradation trajectory with associated weights. The mean RUL estimation is given by the weighted sum of the RUL estimation of each simulated trajectory. Based on the obtained RUL information, advance warning of the battery failure can be achieved and preventive maintenance of the battery can be scheduled so as to improve the availability and reliability of the battery-powered system.

To show how the method can be applied, we conducted case studies. It was found that the proposed approach performed better than the traditional methods. Compared to the mean averaging method, the prediction accuracy at 250 cycles for battery B4 was

improved by 24 cycles when using the DST to define the initial model parameters. In addition, by using the BMC, the mean RUL estimation for the battery B4 was improved by 45 cycles in the accuracy as compared to the extended Kalman filter. Therefore, the capacity fade model can efficiently converges to the battery degradation trend by using the proposed parameter estimation approach, and accurate RUL predictions can be achieved from an early point of the battery life. Another merit of the proposed method is that the RUL prediction can be given in a form of probability distribution, so that the confidence level of the prediction can be assessed. The narrower RUL PDF indicates a higher prediction confidence.

The contributions of this study can be summarized in three points: the first is a new model for the capacity degradation of lithium-ion batteries. This model can well characterize the nonlinear trend of capacity fade and is simple enough for on-board applications. Using this model and the proposed parameter estimation method in this paper, accurate RUL prediction can be achieved from an early point of the battery's life. The second is a novel method based on DST to solve the model initialization problem, which is common for parameter estimation algorithms in battery modeling, including least square, Kalman filter, and BMC. Traditionally, the initial parameter is selected randomly or based on experience. However, poor initial parameters can make the estimation converge slowly or even diverge. This research provides a simple but effective parameter initializing method based on DST. The third is a Bayesian Monte Carlo approach adopted to estimate the model parameters and provide the RUL prediction. This method can take into account the measurement noise and dynamically update the model parameters based on new measurements so as to provide accurate estimations. The improvements of the BMC over the commonly used extended Kalman filter in parameter estimation can be seen from the comparison study. The BMC can also be applied to other estimation and identification problems in the battery research.

This work is an initial effort towards a comprehensive PHM solution for lithium-ion batteries. It has limitations and needs improvement. For example, the effects of capacity gain during battery rest periods were not considered in this study. The models for the effects of rest should be incorporated into the prognostic framework in the future work.

Acknowledgements

The authors would like to thank the more than 100 companies and organizations that support research activities at the Center for Advanced Life Cycle Engineering (CALCE) at the University of Maryland annually. The authors would also like to thank the members of the Prognostics and Health Management Consortium at CALCE for their support of this work.

References

[1] A. Patil, V. Patil, D. Wook Shin, J. Choi, D. Paik, S. Yoon, Materials Research Bulletin 43 (2008) 1913–1942.
[2] I.S. Kim, IEEE Transactions on Power Electronics 25 (2010) 1013–1022.
[3] M. Dubarry, B.Y. Liaw, Journal of Power Sources 194 (2009) 541–549.
[4] IEEE Std. 1188-2005 IEEE Recommended Practices for Maintenance, Testing and Replacement of Valve Regulated Lead-Acid (VRLA) Batteries in Stationary Applications.
[5] S. Cheng, M. Azarian, M. Pecht, Sensors 10 (2010) 5774–5797.
[6] J. Gu, D. Barker, M. Pecht, Microelectronics Reliability 47 (2007) 1849–1856.
[7] M. Pecht, A. Dasgupta, Journal of the Institute of Environmental Sciences 38 (1995) 30–34.
[8] M. Pecht, in: Prognostics and Health Management of Electronics, Wiley-Interscience, New York, 2008.
[9] S. Cheng, K. Tom, L. Thomas, M. Pecht, Sensors Journal, IEEE 10 (2010) 856–862.
[10] J. Kozlowski, 2003 IEEE Aerospace Conference Proceedings, Big Sky, Montana, 2003, pp. 3257–3270.
[11] W.L. Burgess, Journal of Power Sources 191 (2009) 16–21.
[12] B. Saha, K. Goebel, S. Poll, J. Christophersen, IEEE Transactions on Instrumentation and Measurement 58 (2009) 291–296.
[13] K. Goebel, B. Saha, A. Saxena, J. Celaya, J. Christophersen, Instrumentation and Measurement Magazine, IEEE 11 (2008) 33–40.
[14] B. Ayyub, G. Klir, in: Uncertainty Modeling and Analysis in Engineering and the Sciences, Chapman & Hall/CRC, Boca Raton, FL, 2006.
[15] G. Shafer, in: A Mathematical Theory of Evidence, Princeton University Press, Princeton, NJ, 1976.
[16] R.R. Murphy, IEEE Transactions on Robotics and Automation 14 (2002) 197–206.
[17] O. Basir, X. Yuan, Information Fusion 8 (2007) 379–386.
[18] T. Inagaki, IEEE Transactions on Reliability 40 (2002) 182–188.
[19] M. Beynon, B. Curry, P. Morgan, Omega 28 (2000) 37–50.
[20] M. Bauer, International Journal of Approximate Reasoning 17 (1997) 217–237.
[21] M. Beynon, D. Cosker, D. Marshall, Expert Systems with Applications 20 (2001) 357–367.
[22] M.S. Arulampalam, S. Maskell, N. Gordon, T. Clapp, IEEE Transactions on Signal Processing 50 (2002) 174–188.
[23] F. Cadini, E. Zio, D. Avram, Probabilistic Engineering Mechanics 24 (2009) 367–373.
[24] A. Doucet, S. Godsill, C. Andrieu, Statistics and Computing 10 (2000) 197–208.
[25] G.L. Plett, Journal of Power Sources 134 (2004) 277–292.
[26] G.L. Plett, Journal of Power Sources 196 (2011) 2319–2331.
[27] J. Zhang, L. Lee, Journal of Power Sources 196 (2011) 6007–6014.
[28] J. Vetter, P. Novák, M.R. Wagner, C. Veit, K.C. Möller, J.O. Besenhard, M. Winter, M. Wohlfahrt-Mehrens, C. Vogler, A. Hammouche, Journal of Power Sources 147 (2005) 269–281.
[29] Q. Zhang, R.E. White, Journal of Power Sources 179 (2008) 793–798.
[30] R.B. Wright, C.G. Motloch, J.R. Belt, J.P. Christophersen, C.D. Ho, R.A. Richardson, I. Bloom, S.A. Jones, V.S. Battaglia, G.L. Henriksen, T. Unkelhaeuser, D. Ingersoll, H.L. Case, S.A. Rogers, R.A. Sutula, Journal of Power Sources 110 (2002) 445–470.
[31] J.P.M. de Sá, in: Applied Statistics Using SPASS, Statistica and MATLAB, Springer-Verlag, Berlin, Germany, 2003.
[32] S. Ferson, V. Kreinovich, Representation, propagation, and aggregation of uncertainty, SAND Report, 2002.